

Exemestane's 17-hydroxylated metabolite exerts biological effects as an androgen

Eric A. Ariazi,^{1,2} Andrei Leitão,³ Tudor I. Oprea,³ Bin Chen,¹ Teresa Louis,¹ Anne Marie Bertucci,¹ Catherine G.N. Sharma,² Shaun D. Gill,² Helen R. Kim,² Heather A. Shupp,² Jennifer R. Pyle,² Alexis Madrack,² Anne L. Donato,² Dong Cheng,¹ James R. Paige,¹ and V. Craig Jordan^{1,2}

¹Robert H. Lurie Comprehensive Cancer Center, Northwestern University Feinberg School of Medicine, Chicago, Illinois; ²Fox Chase Cancer Center, Philadelphia, Pennsylvania; and ³Division of Biocomputing, University of New Mexico Health Sciences Center, Albuquerque, New Mexico

Abstract

Aromatase inhibitors (AI) are being evaluated as long-term adjuvant therapies and chemopreventives in breast cancer. However, there are concerns about bone mineral density loss in an estrogen-free environment. Unlike nonsteroidal AIs, the steroidal AI exemestane may exert beneficial effects on bone through its primary metabolite 17-hydroexemestane. We investigated 17-hydroexemestane and observed it bound estrogen receptor α (ER α) very weakly and androgen receptor (AR) strongly. Next, we evaluated 17-hydroexemestane in MCF-7 and T47D breast cancer cells and attributed dependency of its effects on ER or AR using the antiestrogen fulvestrant or the antiandrogen bicalutamide. 17-Hydroexemestane induced proliferation, stimulated cell cycle progression and regulated transcription at high sub-micromolar and micromolar concentrations through ER in both cell lines, but through AR at low nanomolar concentrations selectively in T47D cells. Responses of

each cell type to high and low concentrations of the non-aromatizable synthetic androgen R1881 paralleled those of 17-hydroexemestane. 17-Hydroexemestane down-regulated ER α protein levels at high concentrations in a cell type-specific manner similarly as 17 β -estradiol, and increased AR protein accumulation at low concentrations in both cell types similarly as R1881. Computer docking indicated that the 17 β -OH group of 17-hydroexemestane relative to the 17-keto group of exemestane contributed significantly more intermolecular interaction energy toward binding AR than ER α . Molecular modeling also indicated that 17-hydroexemestane interacted with ER α and AR through selective recognition motifs employed by 17 β -estradiol and R1881, respectively. We conclude that 17-hydroexemestane exerts biological effects as an androgen. These results may have important implications for long-term maintenance of patients with AIs. [Mol Cancer Ther 2007;6(11):2817–27]

Introduction

The third-generation aromatase inhibitors (AI) anastrozole (Arimidex; refs. 1, 2), letrozole (Femara; refs. 3, 4), and exemestane (Aromasin; refs. 5, 6), by virtue of blocking extragonadal conversion of androgens to estrogens and giving rise to an estrogen-depleted environment, exhibit improved efficacy over tamoxifen in the adjuvant therapy of estrogen receptor (ER)-positive breast cancer in postmenopausal women (7). Clinical trials evaluating these AIs showed a reduced incidence of contralateral primary breast cancer in the AI groups compared with tamoxifen (1–6); hence, AIs are currently being evaluated as chemopreventives in ongoing studies (8). AIs also exhibit reduced overall toxicity compared with tamoxifen (1–6, 9), but the toxicity profiles are different: tamoxifen is associated with increased incidences of thromboembolic events and endometrial cancer, whereas AIs are associated with decreased bone mineral density (BMD), coupled with an increased risk of bone fractures (10–12) and severe musculoskeletal pain that limits patient compliance (13, 14). Because the available third-generation AIs all exhibit similar efficacies, the selection of a specific AI for long-term adjuvant therapy of breast cancer and as a chemopreventive in healthy women at high risk for breast cancer will likely be determined by safety and tolerability profiles.

AIs fall into two classes, steroidal as represented by exemestane, which acts as a suicide inhibitor of aromatase, and nonsteroidal including anastrozole and letrozole, which reversibly block aromatase activity (7). Possibly due to its steroid structure, exemestane may exhibit a unique pharmacology distinct from the nonsteroidal AIs. In two preclinical studies by Goss et al. (15, 16), exemestane was given to female ovariectomized rats, an animal model

Received 5/3/07; revised 8/28/07; accepted 10/1/07.

Grant support: Department of Defense Breast Program under award BC050277 Center of Excellence (V.C. Jordan; views and opinions of, and endorsements by the author(s) do not reflect those of the U.S. Army or the Department of Defense), Specialized Programs of Research Excellence in Breast Cancer CA89018 (V.C. Jordan), the Avon Foundation (V.C. Jordan), the Weg Fund (V.C. Jordan), and NIH P30 CA006927 (Fox Chase Cancer Center), an Eli Lilly Fellowship (Robert H. Lurie Comprehensive Cancer Center), the Lynn Sage Breast Cancer Research Foundation (Robert H. Lurie Comprehensive Cancer Center), the NIH Molecular Libraries Initiative award U54 MH074425-01, and by National Cancer Institute CA118100 (University of New Mexico Cancer Center).

The costs of publication of this article were defrayed in part by the payment of page charges. This article must therefore be hereby marked *advertisement* in accordance with 18 U.S.C. Section 1734 solely to indicate this fact.

Requests for reprints: V. Craig Jordan, Alfred G. Knudson Chair of Cancer Research, Fox Chase Cancer Center, 333 Cottman Avenue, Philadelphia, PA 19111-2497. Phone: 215-728-7410; Fax: 215-728-7034. E-mail: v.craig.jordan@fccc.edu

Copyright © 2007 American Association for Cancer Research.

doi:10.1158/1535-7163.MCT-07-0312

of osteoporosis, and found to reduce bone resorption markers and increase BMD and bone strength, whereas lowering serum cholesterol and low-density lipoprotein levels compared with ovariectomized controls. One of these preclinical studies also evaluated the nonsteroidal AI letrozole, but in contrast, found no benefit of letrozole on bone or lipid profiles (16). In a clinical study investigating the effects of 2 years of exemestane on bone compared with placebo without prior tamoxifen therapy in patients with surgically resected breast cancer at low risk for recurrence, exemestane did not enhance BMD loss in lumbar spine and only modestly enhanced BMD loss in the femoral neck compared with the placebo group (17). Interestingly, in this study, exemestane promoted bone metabolism by increasing levels of both bone resorption and formation markers (17). However, a clear-cut advantage of exemestane versus the nonsteroidal AIs on bone safety has not been shown in humans, possibly because all other clinical studies compared the AI to tamoxifen (9, 12, 18) or the AI to placebo with prior tamoxifen therapy (10, 11). Drawing conclusions from these studies is difficult because tamoxifen preserves BMD, thereby protecting against fractures, and withdrawal of tamoxifen may have lasting effects on BMD (19).

Maintenance of BMD in women is a known estrogenic effect (20). However, androgen receptors (AR) are also expressed in multiple bone cell types (21, 22), and studies show that androgens maintain BMD in ovariectomized rats (23, 24) and in women (21, 25–27). In ovariectomized rats, physiologic concentrations of androstenedione, a weak androgen and a substrate of aromatase, reduced loss of bone, and the antiandrogen bicalutamide abrogated this effect (23), but anastrozole did not (23). Therefore, the protective effect of androstenedione on maintenance of BMD was androgen mediated and not due to aromatization of androstenedione to estrogen. Furthermore, the non-aromatizable androgen 5 α -dihydrotestosterone has been shown to stimulate bone growth in osteopenic ovariectomized rats (24). In pre- and postmenopausal women, endogenous androgen levels correlate with BMD (25, 26). Furthermore, a study comparing estrogen to a synthetic androgen in postmenopausal osteoporotic women showed that both steroids were equally effective in reducing bone resorption (27). Also, a 2-year double-blind trial showed that estrogen plus a non-aromatizable androgen significantly improved BMD over estrogen alone in surgically menopausal women (28). Therefore, exogenous androgens promote BMD maintenance in women when used alone (27) and in conjunction with estrogen (28).

Although exemestane does not bind ER, it is structurally related to androstenedione and has weak affinity for AR (29, 30). At high doses, exemestane exerts possible androgenic activity *in vivo* by inducing an increase in ventral prostate weight in immature castrated rats (29). Recently, Miki et al. (22) showed in human osteoblast hFOB and osteosarcoma Saos-2 cells that exemestane promoted proliferation, which was partially blocked by the antiandrogen hydroxyflutamide, and increased alkaline phosphatase activity. However, metabolites of exemestane may

be mediating these effects. Exemestane is given p.o. at 25 mg/day and rapidly absorbed, showing peak plasma levels within 2 to 4 h and a direct relationship between dosage and peak plasma levels after single (10–200 mg) or repeated doses (0.5–50 mg; refs. 30, 31). Single-dose studies suggested that exemestane has a short elimination half-life, but multiple-dose studies show its terminal half-life to be about 24 h. Exemestane undergoes complex metabolism, and the primary metabolite in plasma has been identified as 17-hydroxemestane, which accumulates to a concentration of about 10% of its parent compound (30). Taking the possible action of metabolites into consideration, Goss et al. (16) administered 17-hydroxemestane to ovariectomized rats and found that it produced the same bone-sparing effects and favorable changes in circulating lipid levels as exemestane. Also, Miki et al. (22) stated that 17-hydroxemestane promoted proliferation of the osteoblast and osteosarcoma cells similar to exemestane, but the data were not shown, and the authors did not further explore 17-hydroxemestane activities. Additionally, Miki et al. (22) showed that the osteoblasts efficiently metabolized androstenedione to testosterone, which involves the reduction of the 17-keto group of androstenedione to a hydroxyl group. Similar metabolism would convert exemestane to 17-hydroxemestane, and thus, activities of exemestane in the osteoblasts may have been mediated by a metabolite of exemestane. Hence, a thorough investigation of exemestane and 17-hydroxemestane activities through ER and AR is warranted to provide evidence regarding whether exemestane could display a more favorable safety and toxicity profile than nonsteroidal AIs for long-term adjuvant use and as a chemopreventive of breast cancer in postmenopausal women. Therefore, we evaluated the pharmacologic actions of exemestane and its primary metabolite 17-hydroxemestane on ER- and AR-regulated activities in a range of cellular and molecular assays. First, we determined the relative binding affinity (RBA) of 17-hydroxemestane to ER α and AR. Next, using MCF-7 and T47D breast cancer cells, we examined the ability of 17-hydroxemestane to stimulate cell proliferation and cell cycle progression (Supplementary Material)⁴ via ER and AR, to regulate ER- and AR-dependent transcription, and to modulate ER α and AR protein levels. Lastly, we investigated intermolecular interactions between 17-hydroxemestane and ER α and AR using molecular modeling.

Materials and Methods

Compounds and Cell Lines

Exemestane and 17-hydroxemestane were provided by Pfizer. Fulvestrant (ICI 182,780, Faslodex) and bicalutamide (Casodex) were provided by Dr. Alan E. Wakeling and Dr. Barrington J.A. Furr (AstraZeneca Pharmaceuticals, Macclesfield, United Kingdom), respectively. All other

⁴ Supplementary material for this article is available at Molecular Cancer Therapeutics Online (<http://mct.aacrjournals.org/>).

compounds were obtained from Sigma-Aldrich, and cell culture reagents were from Invitrogen. All test agents were dissolved in ethanol and added to the medium at 1:1,000 (v/v). MCF-7/WS8 and T47D:A18 human mammary carcinoma cells, clonally selected from their parental counterparts for sensitivity to growth stimulation by E₂ (32), were used in all experiments indicating MCF-7 and T47D cells. Cells were maintained in steroid-replete RPMI 1640, but 3 days before all experiments, were cultured in steroid-free media as previously described (32, 33).

Competitive Hormone-Binding Assays

Competitive hormone-binding assays were conducted using fluorescence polarization-based ER α and AR Competitor Assay kits (Invitrogen) as previously described (34).

Cellular Proliferation Assays

Cellular proliferation following 7 days in culture was determined by DNA mass per well in 12-well plates using the fluorescent DNA dye Hoechst 33258 as previously described (32).

Reporter Gene Assays

Reporter gene assays were conducted by transfecting cells with either an ERE(5x)-regulated (pERE(5x)TA-ffLuc; ref. 33) or ARE(5x)-regulated (pAR-Luc; Panomics) firefly luciferase expression plasmid and co-transfected with a basal TATA promoter-regulated (pTA-srLuc) *Renilla* luciferase expression plasmid as previously described (33).

Quantitative Real-Time PCR

Quantitative real-time PCR (qPCR) was used to determine AR and ribosomal large phosphoprotein subunit P0 (RLP0; 36B4) mRNA levels as previously described (35).

Immunoblot Analyses

Immunoblots, prepared as previously described (33), were probed with primary antibodies against AR (AR 441; Lab Vision), ER α (AER 611; Lab Vision), and β -actin (AC-15; Sigma-Aldrich).

Molecular Modeling and Virtual Docking Calculations

The three-dimensional conformations for E₂, 17-hydroexemestane, exemestane, R1881, and dexamethasone were generated with Omega version 2.1 software (OpenEye Scientific Software). These compounds were docked using the following X-ray crystallographic structures: 1GWR (ER α co-complexed with E₂, 2.4-Å resolution; ref. 36) and 1XQ3 (AR co-complexed with R1881, 2.25-Å resolution; ref. 37). ER α and AR ligand-binding pockets were built using a ligand-centered box and the receptor-bound conformation of the respective ligand: E₂ (for 1GWR) and R1881 (for 1XQ3). The volume of the cavity differs for the two receptors: 648 Å³ for 1GWR and 532 Å³ for 1XQ3. All receptor and ligand bonds were kept rigid. The receptor structures were filled with water because ER α (38) and AR crystal structures (39) indicate that specific stable hydrogen bond (H-bond) networks form among particular water molecules, ligands, and amino acid side chains. Docking was done with FRED version 2.2 software (OpenEye) using a short refinement step for the ligands within the receptor and using the MMFF94 force field. The best 30 conformations for each compound were compared and ranked by FRED's Chemscore function. For each ligand-

docked receptor evaluated, the docked conformation with the lowest total intermolecular interaction energy (kJ/mol) was selected. To address whether water could be displaced by a compound during the process of binding, docking calculations were also done using receptors modeled with water removed as presented in Supplementary Table S1⁴ and the differences between the methods in Supplementary Table S2.⁴

Curve Fitting and Statistical Analyses

All statistical tests, curve fitting, and determination of half-maximal inhibitory concentrations (IC₅₀) and half-maximal effective concentrations (EC₅₀) were done using GraphPad Prism 4.03 (GraphPad Software). Significant differences were determined using one-way ANOVA with Bonferroni multiple comparison post-test.

Results

Experimentally Determined Binding of 17-Hydroexemestane and Exemestane to ER α and AR

Structures of the compounds relevant to these studies, the steroidal AI parent compound exemestane, its primary metabolite 17-hydroexemestane, E₂, and the synthetic non-aromatizable androgen R1881, are shown in Fig. 1A. Importantly, the only difference between parental exemestane and its metabolite 17-hydroexemestane is a hydroxyl group in the metabolite in place of a ketone in the parent compound at the 17 β position, whereas both compounds share a 3-keto group. For steroidal estrogens, elimination or modification of the 17 β -OH group reduces binding to ER α , but that of the 3-OH group is much more dramatic (40). For steroidal androgens, the trend is reversed; elimination or modification of the 17 β -OH group is more significant for AR binding than that of the 3-keto group (41). The 3-keto group found in both exemestane and 17-hydroexemestane also favors binding to AR (41).

We tested the binding of exemestane and 17-hydroexemestane to ER α and AR using fluorescence polarization-based competitive hormone-binding assays (Fig. 1B and C; Table 1). For purposes of comparison, compound affinities were arbitrarily categorized with respect to their RBAs as strong (100 to ≥ 1), moderate (<1 to ≥ 0.1), weak (<0.1 to ≥ 0.01), very weak (<0.01 to detectable binding defined as 50% competition), and inactive (compound did not compete for at least 50% binding). E₂ competitively bound ER α with an IC₅₀ of 1.33×10^{-9} mol/L (RBA = 100; Fig. 1B), and R1881 competitively bound AR with an IC₅₀ of 1.34×10^{-8} mol/L (RBA = 100; Fig. 1C). Considering ER α (Fig. 1B), both R1881 and 17-hydroexemestane competed for binding to ER α with IC₅₀s of 1.02×10^{-6} mol/L (RBA = 0.130) and 2.12×10^{-5} mol/L (RBA = 0.006), respectively, which categorized R1881 as a moderate and 17-hydroexemestane as a very weak ER α ligand. Neither exemestane nor dexamethasone significantly competed for binding to ER α . Regarding AR (Fig. 1C), 17-hydroexemestane and exemestane competed for binding to AR with IC₅₀s of 3.96×10^{-8} mol/L (RBA = 33.8) and 2.03×10^{-6} mol/L (RBA = 0.658), respectively, which classified

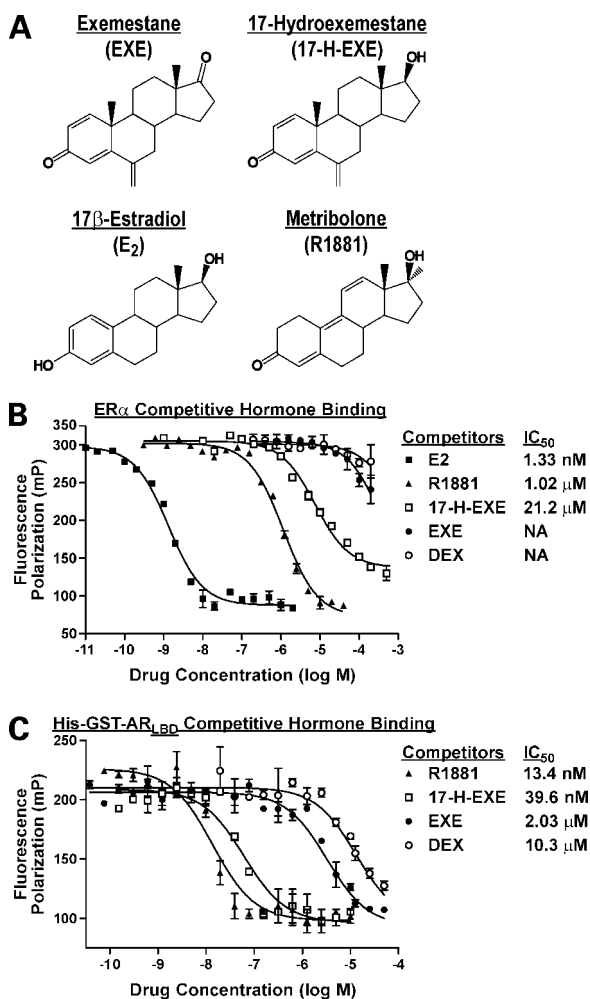


Figure 1. Compounds examined in this study and their RBAs for ER α and AR. **A**, structures of exemestane, its primary metabolite 17-hydroxemestane E₂, and R1881. ER α (**B**) and AR (**C**) fluorescence polarization-based competitive hormone-binding assays. Baculovirus-produced human ER α and rat AR ligand-binding domain tagged with a His-glutathione S-transferase epitope (His-GST-AR_{LBD}) were used at final concentrations of 15 and 25 nmol/L, respectively. The fluorescently labeled ER α and AR ligands, Fluormone ES2 and Fluormone AL Green, respectively, were both used at a final concentration of 1 nmol/L. The competing test compounds were E₂, R1881, 17-hydroxemestane, exemestane, and dexamethasone (DEX) as indicated. *Point*, mean of triplicate determinations; *bars*, 95% confidence intervals. Curve fitting was done using GraphPad Prism software (version 4.03). IC₅₀s corresponding to a half-maximal shift in polarization values of the test compounds were determined using the maximum and minimum polarization values of the E₂-competitive binding curve for ER α or of the R1881-competitive binding curve for AR as appropriate.

17-hydroxemestane as a strong and exemestane as a weak AR ligand. However, dexamethasone would also be categorized as a weak AR ligand. Hence, the observed very weak ER α binding and strong AR binding of 17-hydroxemestane was consistent with what previously reported structure-activity relationships (40, 41) would have predicted due to reduction of the 17-keto group in exemestane to a 17 β -OH in the metabolite.

Proliferation Responses to 17-Hydroxemestane and Exemestane

We examined the effects of exemestane and 17-hydroxemestane on 7 days of proliferation in ER α - and AR-positive MCF-7 and T47D mammary carcinoma cells (Fig. 2). As expected, both cell lines were growth stimulated by E₂, with growth EC₅₀s of 1.7×10^{-12} mol/L E₂ for MCF-7 cells (Fig. 2A) and 7.1×10^{-12} mol/L E₂ for T47D cells (Fig. 2B). These growth responses to E₂ were completely blocked by fulvestrant (all *P* values <0.001), validating the E₂ responsiveness via ER in these cell lines.

Both cell lines were also growth stimulated by R1881 (Fig. 2A and B) and 17-hydroxemestane (Fig. 2C and D), whereas exemestane did not exert any significant effect on proliferation (Fig. 2C and D). Considering MCF-7 cells, R1881 exhibited a growth EC₅₀ of 2.4×10^{-8} mol/L (Fig. 2A), or approximately 4 orders of magnitude higher than that of E₂. Similarly, 17-hydroxemestane exhibited a growth EC₅₀ of 2.7×10^{-6} mol/L in MCF-7 cells (Fig. 2C) or approximately 6 orders of magnitude higher than that of E₂. These growth responses to R1881 and 17-hydroxemestane in MCF-7 cells were completely blocked by cotreatment with fulvestrant (Fig. 2A and B; both *P* values <0.001). Therefore, whereas R1881, a non-aromatizable synthetic androgen, stimulated growth of MCF-7 cells, it did so by acting through ER. Hence, at high concentrations, R1881 exerted estrogenic activity. Similarly, at high concentrations, 17-hydroxemestane also exerted estrogenic activity and stimulated growth of MCF-7 cells by acting through ER.

Interestingly, in T47D cells, the growth response to R1881 and 17-hydroxemestane followed an apparent bimodal pattern, which was different than in MCF-7 cells. In T47D cells, proliferative effects of high concentrations of R1881 (5×10^{-6} mol/L; Fig. 2B) and 17-hydroxemestane (5×10^{-6} mol/L; Fig. 2D) were only partially blocked by fulvestrant (both *P* values <0.001), down to the level of growth observed at nanomolar concentrations of these compounds. However, proliferative effects of lower concentrations of R1881 (10^{-9} mol/L) and 17-hydroxemestane (10^{-8} mol/L) were completely blocked by the anti-androgen bicalutamide (both *P* values <0.001). Based on these observed levels of inhibition by bicalutamide and fulvestrant, maximal concentrations at which R1881 and 17-hydroxemestane stimulated growth through AR-dependent activities were 10^{-7} and 10^{-6} mol/L, respectively, and above these concentrations, R1881 and 17-hydroxemestane stimulated growth through ER-dependent activities. Using this information to define concentration ranges in which these compounds exert AR-mediated or ER-mediated effects in T47D cells, the growth EC₅₀s via AR of R1881 and 17-hydroxemestane were 1.0×10^{-10} mol/L (Fig. 2B) and 4.3×10^{-10} mol/L (Fig. 2D), respectively. Similarly, the growth EC₅₀s via ER of R1881 and 17-hydroxemestane in T47D cells were 3.1×10^{-7} mol/L (Fig. 2B) and 1.5×10^{-6} mol/L (Fig. 2D), respectively. Hence, in T47D cells, both R1881 and 17-hydroxemestane stimulated growth via AR at lower

concentrations and via ER at higher concentrations. These results were consistent with the observed binding affinities of these compounds to ER α (Fig. 1B) and AR (Fig. 1C).

Cell Cycle Progression Responses to 17-Hydroxexemestane

As shown in Supplementary Fig. S1,⁴ 17-hydroxexemestane at 10^{-8} mol/L acted through AR to stimulate S-phase entry in T47D cells by 1.9-fold ($P < 0.001$) but, at 5×10^{-6} mol/L, acted through ER to stimulate S-phase entry in MCF-7 cells by 2.2-fold ($P < 0.001$). Hence, 17-hydroxexemestane effects on cell cycle progression were consistent with its effects on proliferation (Fig. 2).

Regulation of ER α and AR Transcriptional Activities by 17-Hydroxexemestane

Next, we investigated the ability of 17-hydroxexemestane to regulate ER and AR transcriptional activity by transfecting cells with an ERE(5x)-regulated or ARE(5x)-regulated dual-luciferase plasmid set, treating cells with test compounds, and measuring dual-luciferase activity 44 h after treatment (Fig. 3A–C). E₂ at 10^{-10} mol/L induced ERE(5x)-regulated transcription by 19.4-fold in MCF-7 cells (Fig. 3A; $P < 0.001$), and 11.3-fold in T47D cells (Fig. 3B; $P < 0.001$) compared with control-treated cells; this E₂-induced transcriptional activity was blocked by fulvestrant (both P values < 0.001), validating dependence on ER for ERE(5x)-regulated transcription. At high sub-micromolar and micromolar concentrations, R1881 stimulated ERE(5x)-regulated transcription in both cell lines, with maximal inductions of 22.7-fold at 5×10^{-6} mol/L in MCF-7 cells (Fig. 3A; $P < 0.001$), and 7.9-fold at 5×10^{-6} mol/L in T47D cells (Fig. 3B; $P < 0.001$) compared with control-treated cells. The ability of R1881 at 5×10^{-6} mol/L to induce ERE(5x)-regulated transcription was blocked by fulvestrant (Fig. 3A and B; both P values < 0.001), indicating that at high concentrations, R1881 acted as an estrogen. In a similar manner as R1881, 17-hydroxexemestane stimulated ERE(5x)-regulated transcription in a concentration-dependent manner at sub-micromolar and micromolar concentrations

(Fig. 3A and B). At 5×10^{-6} mol/L, 17-hydroxexemestane maximally induced ERE(5x)-regulated transcription by 7.7-fold in MCF-7 cells (Fig. 3A; $P < 0.001$) and 3.3-fold in T47D cells (Fig. 3B; $P < 0.001$) compared with control-treated cells; this transcriptional activation was blocked by fulvestrant (both P values < 0.001). Therefore, at high concentrations, 17-hydroxexemestane acted as an estrogen and induced ER transcriptional activity.

In a similar manner, AR-dependent transcriptional activity was investigated. T47D cells showed a concentration-dependent induction of ARE(5x)-regulated transcription in response to R1881, with 10^{-9} mol/L R1881 inducing transcription by 8.5-fold and 10^{-6} mol/L R1881 maximally inducing transcription by 12.7-fold relative to control-treated cells (Fig. 3C; both P values < 0.001). Bicalutamide blocked 10^{-9} mol/L R1881-mediated induction of ARE(5x)-regulated transcription (Fig. 3C; $P < 0.001$), confirming dependence on AR. MCF-7 cells failed to respond to 10^{-6} mol/L R1881 with induction of ARE(5x)-regulated transcription (data not shown), although these cells express AR protein. This supports our prior results that T47D cells were growth stimulated by R1881 through an AR-dependent mechanism (Fig. 2B), but that MCF-7 cells were not (Fig. 2A). As expected, 10^{-6} mol/L E₂ failed to induce ARE(5x)-regulated transcription (Fig. 3C). Next, 17-hydroxexemestane was evaluated in T47D cells and, in a concentration-dependent manner, induced ARE(5x)-regulated transcription with maximal induction of 4.7-fold occurring at 5×10^{-6} mol/L relative to control treatment (Fig. 3C; $P < 0.001$). However, because high concentrations of 17-hydroxexemestane were needed to induce this synthetic ARE(5x)-regulated promoter, we tested whether lower concentrations of 17-hydroxexemestane could modulate endogenous AR mRNA expression, which is known to be negatively feedback regulated by its gene product (42). Using real-time PCR, AR mRNA levels were determined in T47D cells following 24 h of treatment with test compounds (Fig. 3D). R1881 at 10^{-9} mol/L significantly down-regulated

Table 1. Compound affinity for ER α and AR determined experimentally using a competitive hormone-binding assay (Fig. 1B and C), and by computer docking in which receptors were modeled as filled with water

Compound	Receptor	Competitive hormone binding			Intermolecular interaction energy (kJ/mol)				
		IC ₅₀ (mol/L)	95% CI (mol/L)	RBA (%)	Total score	Lipophilic	H-bond	Steric clash	RTB penalty
E ₂	ER α	1.33×10^{-9}	$1.18-1.49 \times 10^{-9}$	100	-31.90	-25.96	-6.00	0.06	0
R1881	ER α	1.02×10^{-6}	$0.90-1.15 \times 10^{-6}$	0.130	-29.96	-26.01	-4.32	0.37	0
17-Hydroxexemestane	ER α	2.12×10^{-5}	$1.73-2.61 \times 10^{-5}$	0.006	-29.14	-27.73	-3.34	1.93	0
Exemestane	ER α	NA			-27.33	-25.98	-3.34	1.99	0
Dexamethasone	ER α	NA			-23.71	-29.70	-4.18	9.07	1.10
R1881	AR	1.34×10^{-8}	$1.00-1.79 \times 10^{-8}$	100	-32.75	-28.47	-4.56	0.28	0
17-Hydroxexemestane	AR	3.96×10^{-8}	$2.74-5.71 \times 10^{-8}$	33.8	-31.95	-30.54	-4.76	3.35	0
Exemestane	AR	2.03×10^{-6}	$1.39-2.97 \times 10^{-6}$	0.658	-26.48	-28.80	-2.11	4.43	0
Dexamethasone	AR	1.03×10^{-5}	$0.75-1.43 \times 10^{-5}$	0.130	-24.53	-32.21	-2.49	9.07	1.10

Abbreviations: RTB Penalty, rotatable bond penalty; NA, not applicable; test compound did not compete for at least 50% binding of ER α .

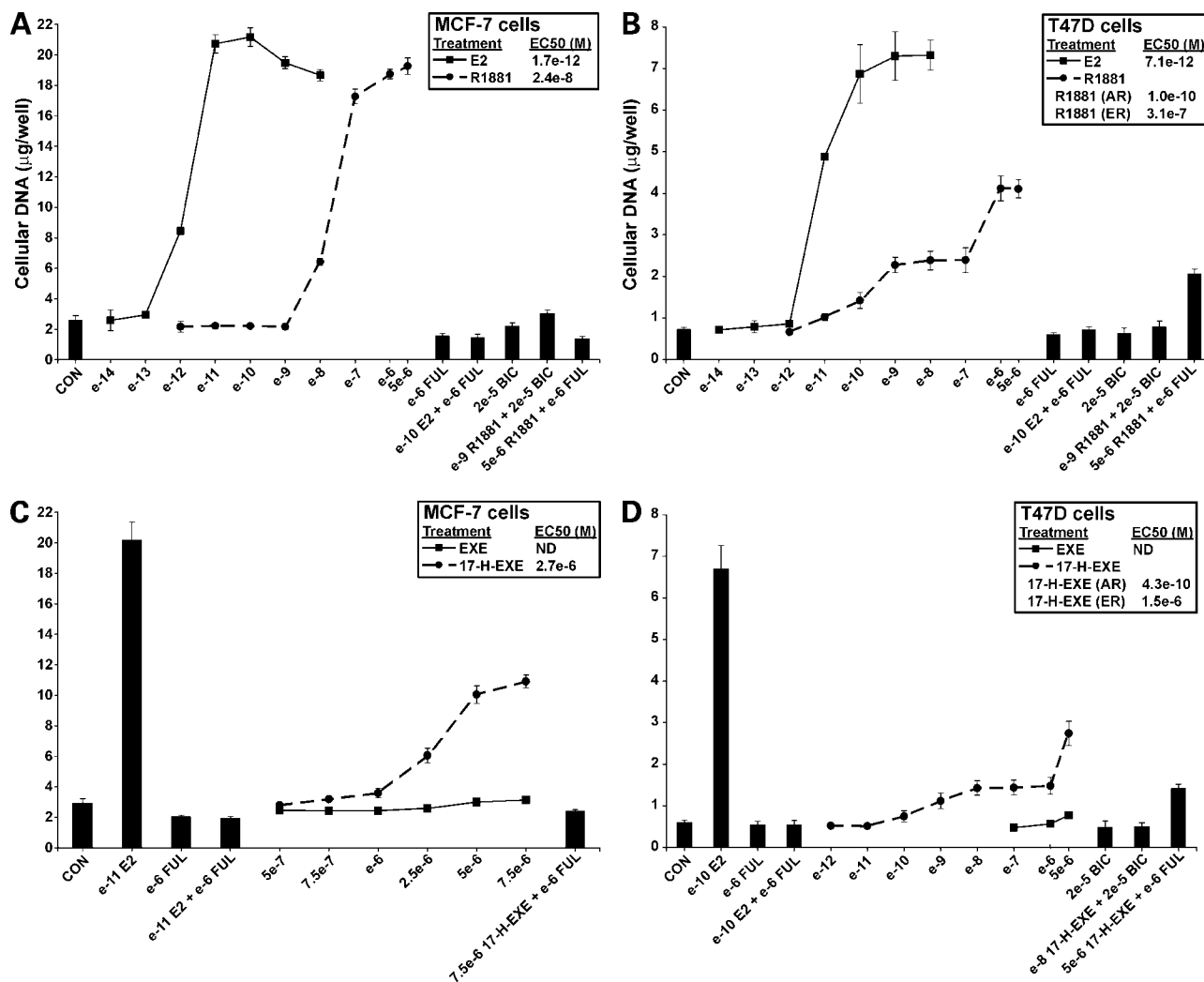


Figure 2. 17-Hydroxemestane and R1881 stimulate cellular proliferation. DNA-based cellular proliferation assays of (A) MCF-7 cells treated with E₂ and R1881, (B) T47D cells treated with E₂ and R1881, (C) MCF-7 cells treated with exemestane and 17-hydroxemestane, and (D) T47D cells treated with exemestane and 17-hydroxemestane. Cells were cultured in steroid-free medium for 3 d before the assays. MCF-7 cells were seeded at 15,000 cells per well and T47D cells at 20,000 cells per well in 12-well plates. Cells were treated on days 0 (the day after seeding), 3, and 6, and then collected on day 7. Cellular DNA quantities were determined using the fluorescent DNA-binding dye Hoechst 33258 and compared against a standard curve. Data shown represent the mean of four replicates and SDs. DNA values were fitted to a sigmoidal dose-response curve and growth EC₅₀s calculated using GraphPad Prism 4.03 software. At high concentrations, 17-hydroxemestane and R1881 increased growth via ER in both cell lines but, at low concentrations, stimulated growth via AR selectively in T47D cells. Abbreviations: CON, control; FUL, fulvestrant; BIC, bicalutamide.

AR mRNA expression by 48% ($P < 0.001$), whereas 10^{-9} mol/L E₂ did not (Fig. 3D). Bicalutamide prevented R1881-mediated decrease in AR mRNA expression (Fig. 3D), validating that AR mRNA levels were negatively feedback regulated. Similarly, a low 10^{-8} mol/L concentration of 17-hydroxemestane led to a 41% decrease in AR mRNA levels ($P < 0.01$), with increased 17-hydroxemestane concentrations further decreasing AR mRNA expression (Fig. 3D). Bicalutamide blocked 17-hydroxemestane-mediated down-regulation of AR mRNA expression ($P < 0.01$), whereas fulvestrant did not (Fig. 3D). Therefore, 17-hydroxemestane acted as an androgen via AR to feedback-regulate the expression of endogenous AR mRNA in T47D cells.

Modulation of AR and ER α Protein Levels by 17-Hydroxemestane

Androgens and estrogens modulate protein expression levels of their cognate receptors. R1881 stabilizes AR protein allowing its accumulation (43), whereas E₂ promotes ER α degradation in a cell type-dependent manner (32). Therefore, we investigated the effects of 17-hydroxemestane on AR and ER α protein levels by treating cells with test compounds for 24 h and analyzing receptor levels by immunoblotting. E₂ decreased ER α protein levels in MCF-7 (Fig. 4A), but not T47D cells (Fig. 4B), as we have previously shown (32). As expected, fulvestrant promoted ER α protein degradation in both cell lines. E₂ did not significantly affect AR protein accumulation in MCF-7 cells

(Fig. 4A), but did down-regulate AR protein levels in T47D cells (Fig. 4B). Also, fulvestrant and E₂ plus fulvestrant treatments did not significantly affect AR protein levels in MCF-7 cells (Fig. 4A), but did modestly up-regulate AR protein levels in T47D cells (Fig. 4B). As expected, R1881 caused an increase in accumulation of AR protein in both cell lines (Fig. 4A and B), likely by stabilizing the protein (43). Next, we characterized the effects of low 10⁻⁸ mol/L and high 5 × 10⁻⁶ mol/L concentrations of 17-hydroxemestane on ERα and AR expression. The high 5 × 10⁻⁶ mol/L concentration of 17-hydroxemestane led to decreased ERα protein levels in MCF-7 (Fig. 4A), but not in T47D cells (Fig. 4B); this pattern indicates that 5 × 10⁻⁶ mol/L

17-hydroxemestane acted as an estrogen to regulate ERα protein in a cell type-dependent manner. Similar to R1881, treatment with low 10⁻⁸ mol/L or high 5 × 10⁻⁶ mol/L concentrations of 17-hydroxemestane led to increased AR protein accumulation in both cell lines (Fig. 4A and B), indicating that 17-hydroxemestane acted as an androgen likely by stabilizing AR protein. Therefore, 17-hydroxemestane modulated ERα and AR protein accumulation as would an estrogen and an androgen, respectively.

Molecular Docking of 17-Hydroxemestane and Exemestane to ERα and AR

To investigate the mechanism by which 17-hydroxemestane binds ERα as a very weak ligand and AR as a

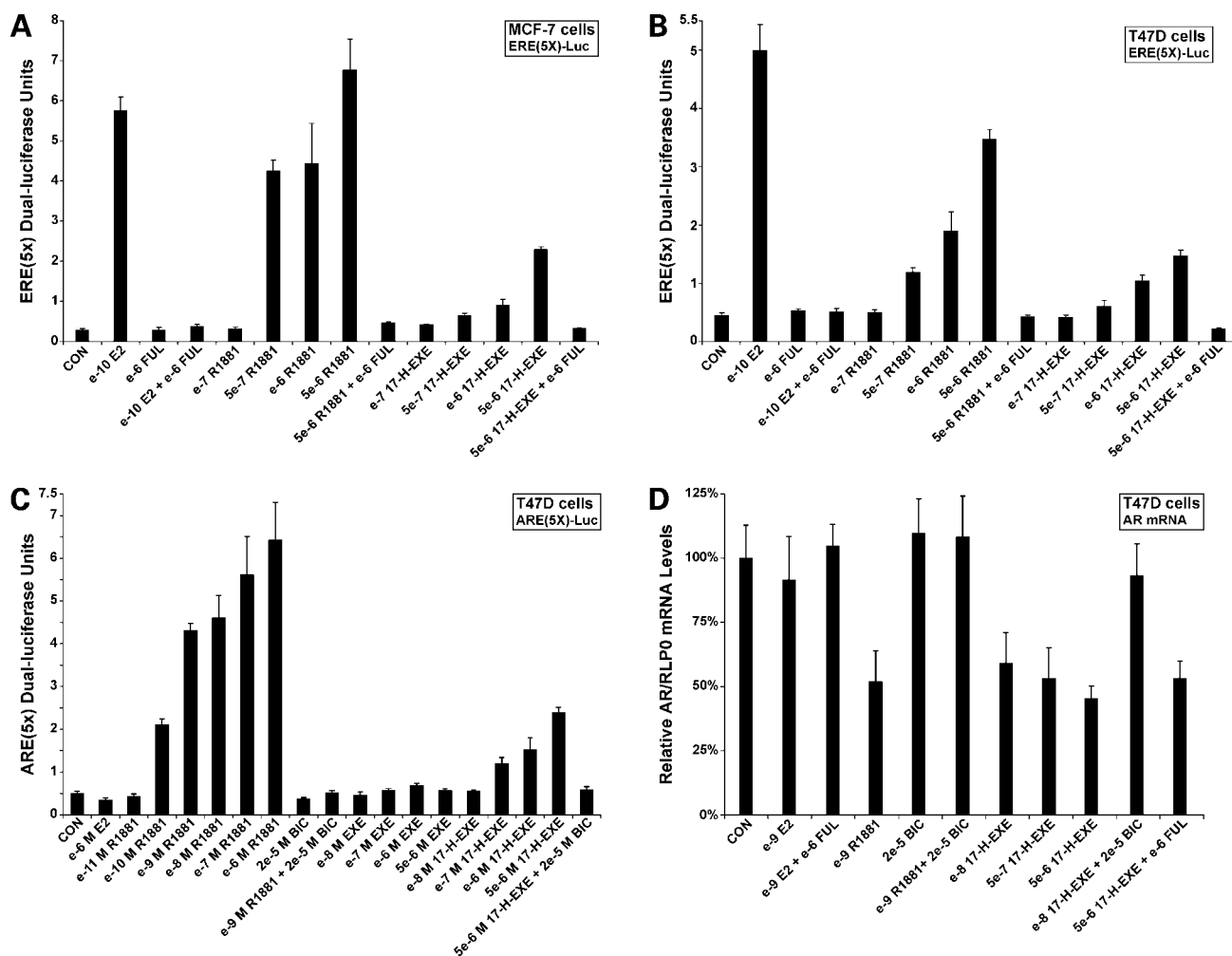


Figure 3. 17-Hydroxemestane and R1881 regulate ER transcriptional activity at high concentrations and AR transcriptional activity at low concentrations. ERE(5x)-regulated dual-luciferase activity in (A) MCF-7 cells and (B) T47D cells. (C) ARE(5x)-regulated reporter gene activity in T47D cells. A–C, Under steroid-free conditions, cells were transiently transfected with pERE(5x)TA-ffLuc or pARE(5x)-Luc (firefly luciferase reporter plasmids) and the internal normalization control pTA-srLuc (*Renilla* luciferase reporter plasmid). Four hours after transfection, cells were treated as indicated and then again the following day. Cells were assayed 44 h after transfection for dual-luciferase activity. Data shown are the mean of triplicate determinations and associated SDs. 17-Hydroxemestane and R1881 stimulated ERE(5x)-regulated transcription in MCF-7 and T47D cells and ARE(5x)-regulated transcriptional activity in T47D cells. D, AR mRNA levels in T47D cells as determined by real-time PCR. T47D cells were treated as indicated for 24 h. RNA was isolated and converted to cDNA. Continuous accumulation of PCR products was monitored using the double strand-specific DNA dye SYBR Green. Quantitative measurements of AR mRNA and the endogenous normalization control RLPO mRNA were determined by comparison to a standard curve of known quantities of serially diluted AR or RLPO PCR product. The data represent the mean and SDs of three independent samples, each of which was measured in triplicate. 17-Hydroxemestane and R1881 down-regulated AR mRNA levels at nanomolar concentrations in an AR-dependent manner.

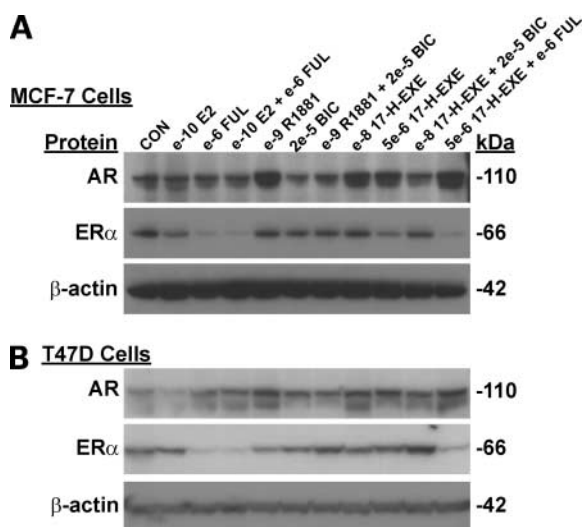


Figure 4. 17-Hydroxexemestane modulates AR and ER α protein levels. Immunoblot analysis of AR and ER α in (A) MCF-7 cells and (B) T47D cells. Cells were treated as indicated for 24 h, and 20 μ g of cellular protein were resolved by 4% to 12% SDS-PAGE and then transferred to a nylon membrane. Membranes were probed for AR, ER α , and β -actin, and immunoreactive bands were visualized by chemiluminescence and autoradiography. Cropped blots are shown. 17-hydroxexemestane up-regulated AR protein levels at 10^{-8} mol/L in both cell lines and down-regulated ER α in MCF-7 cells at 5×10^{-6} mol/L.

strong ligand, molecular models were constructed *in silico*. The trends in the computed intermolecular interaction energies matched the experimentally determined RBAs (Table 1). Superimposition of the docked and crystallographic structures of E $_2$ complexed with ER α (Fig. 5A) and of R1881 complexed with AR (Fig. 5B) showed that the docking models recapitulated the molecular recognition patterns of the crystal structures.

Considering ER α , the intermolecular interaction energies of R1881 and 17-hydroxexemestane were less favorable than E $_2$ by 1.94 and 2.76 kJ/mol, respectively, due to decreased H-bond interactions and increased steric clash (Table 1). Exemestane was much less favorable than E $_2$ by 4.57 kJ/mol (Table 1). Hence, the 17 β -OH group of 17-hydroxexemestane compared with the 17-keto group of exemestane contributed -1.81 kJ/mol toward increased affinity for ER α . Interestingly, the docking calculations suggested that the higher affinity of 17-hydroxexemestane over exemestane for ER α was not due to increased H-bonding mediated by the 17 β -OH group, but rather increased lipophilic interactions (Table 1) due to a slight repositioning of the compound as a consequence of 17 β -OH group. In the E $_2$ docked to ER α model, H-bonds between E $_2$ and Glu 353 , Arg 394 , and His 524 side chains were observed (Fig. 5A). In the docked 17-hydroxexemestane to ER α model (Fig. 5C), the same Arg 394 and His 524 interactions were maintained, except that there was a loss of the Glu 353 interaction. The R1881 docked to ER α model is shown in Supplementary Fig. S2A.⁴

Considering AR, the intermolecular interaction energy of 17-hydroxexemestane was only 0.8 kJ/mol less favorable

than R1881, whereas exemestane was significantly less favorable than R1881 by 6.27 kJ/mol (Table 1). Docking of 17-hydroxexemestane to AR, compared with the parent drug exemestane, indicated that 17-hydroxexemestane exhibited improved lipophilic interactions by -2.11 kJ/mol, more favorable H-bonding interactions by -2.65 kJ/mol, and decreased steric clash by -1.08 kJ/mol. Hence, the 17 β -OH group in 17-hydroxexemestane compared with the 17-keto group in exemestane contributed -5.47 kJ/mol toward higher affinity for binding AR (Table 1). In the R1881 docked to AR model, H-bonds between R1881 and Asn 705 , Gln 711 and Arg 752 were observed (Fig. 5B). The OH side chain of Thr 877 was in close proximity to both docked R1881 (Fig. 5B) and 17-hydroxexemestane (Fig. 5D), but the angle was not favorable for H-bonding. Docking of 17-hydroxexemestane to AR (Fig. 5D) indicated a short 2.78-Å H-bond between the 17 β -OH group of the ligand and Asn 705 , but not between the 3-keto group of the ligand and Gln 711 and Arg 752 . Hence, the short 2.78-Å H-bond observed in the 17-hydroxexemestane docked to AR model was important in mediating high affinity binding. The exemestane docked to AR model is shown in Supplementary Fig. S2B.⁴

Discussion

We observed that 17-hydroxexemestane, the primary metabolite of exemestane, bound to ER α as a very weak ligand and acted through ER at high sub-micromolar and micromolar concentrations to stimulate growth, promote cell cycle progression, induce ERE-regulated reporter gene expression, and down-modulate ER α protein levels in breast cancer cells. However, we also observed that 17-hydroxexemestane bound to AR as a strong ligand and found in T47D cells that 17-hydroxexemestane stimulated growth, induced cell cycle progression, down-modulated AR mRNA expression, and stabilized AR protein levels, with all of these effects occurring at low nanomolar concentrations and blocked by bicalutamide. Moreover, computer docking indicated that the 17 β -OH group of 17-hydroxexemestane versus the 17-keto group of exemestane contributed significantly more toward increasing affinity to AR than to ER α . Molecular modeling also indicated that 17 β -OH group of 17-hydroxexemestane interacted with AR through an important H-bond of Asn 705 , a conserved recognition motif employed by R1881. Therefore, we propose that the primary mechanism of action of exemestane *in vivo* is mediated by 17-hydroxexemestane regulating AR activities.

The Food and Drug Administration label for exemestane (Aromasin; Pfizer) reports that in postmenopausal women with advanced breast cancer, the mean AUC (area under the curve) values of exemestane following repeated doses was 75.4 ng-h/mL (254 nmol-h/L), which was almost twice that in healthy postmenopausal women (41.4 ng-h/mL; 140 nmol-h/L; ref. 31). Because circulating levels of 17-hydroxexemestane can reach about 1/10 the level of the parent compound (30), we hypothesize that circulating levels of 17-hydroxexemestane are sufficient to bind AR and

regulate AR-dependent activities. Furthermore, a subpopulation of patients may exist who metabolize exemestane at higher rates, leading to correspondingly higher circulating 17-hydroexemestane levels. For instance, one of three patients administered 800 mg of exemestane, the highest dose evaluated, achieved 17-hydroexemestane plasma levels approximately one-half the level of the parent compound (30). Based on our results, we would predict that higher circulating levels of 17-hydroexemestane would associate with decreased rates of BMD loss and risk of bone fractures in postmenopausal women. We suggest that circulating levels of 17-hydroexemestane and exemestane should be determined in clinical trials and correlated to disease outcome and toxicity profiles such as BMD loss.

Although the clinical studies reported thus far were not designed to directly compare one AI versus another, comparisons in the rate of BMD loss from baseline to year 1, and from year 1 to 2 can be made. In the bone safety subprotocol of the IES (Intergroup Exemestane Study) trial,

the rate of BMD loss was greatest within 6 months of switching from tamoxifen to exemestane at -2.7% in the lumbar spine and -1.4% in the hip, but thereafter, BMD loss progressively slowed in months 6 to 12 and again in months 12 to 24 to only -1.0% and -0.8% in the lumbar spine and hip, respectively (10), which is in the same range as would be expected for postmenopausal women in general. However, in the bone safety substudy of the MA.17 trial, patients administered letrozole experienced a relatively constant rate of BMD loss for 2 years: at 12 months, the rate of BMD loss from baseline was -3.3% and -1.43% in lumbar spine and hip, respectively, and from year 1 to year 2, -2.05% and -2.17% in lumbar spine and hip, respectively (11). In the bone substudy of the ATAC (Arimidex, Tamoxifen, Alone or in Combination) trial, the rate of BMD loss from baseline to year 1 was -2.2% in lumbar spine and -1.5% in hip and from year 1 to year 2, -1.8% in lumbar spine and -1.9% in hip (18). Collectively, these results suggest that after the initial

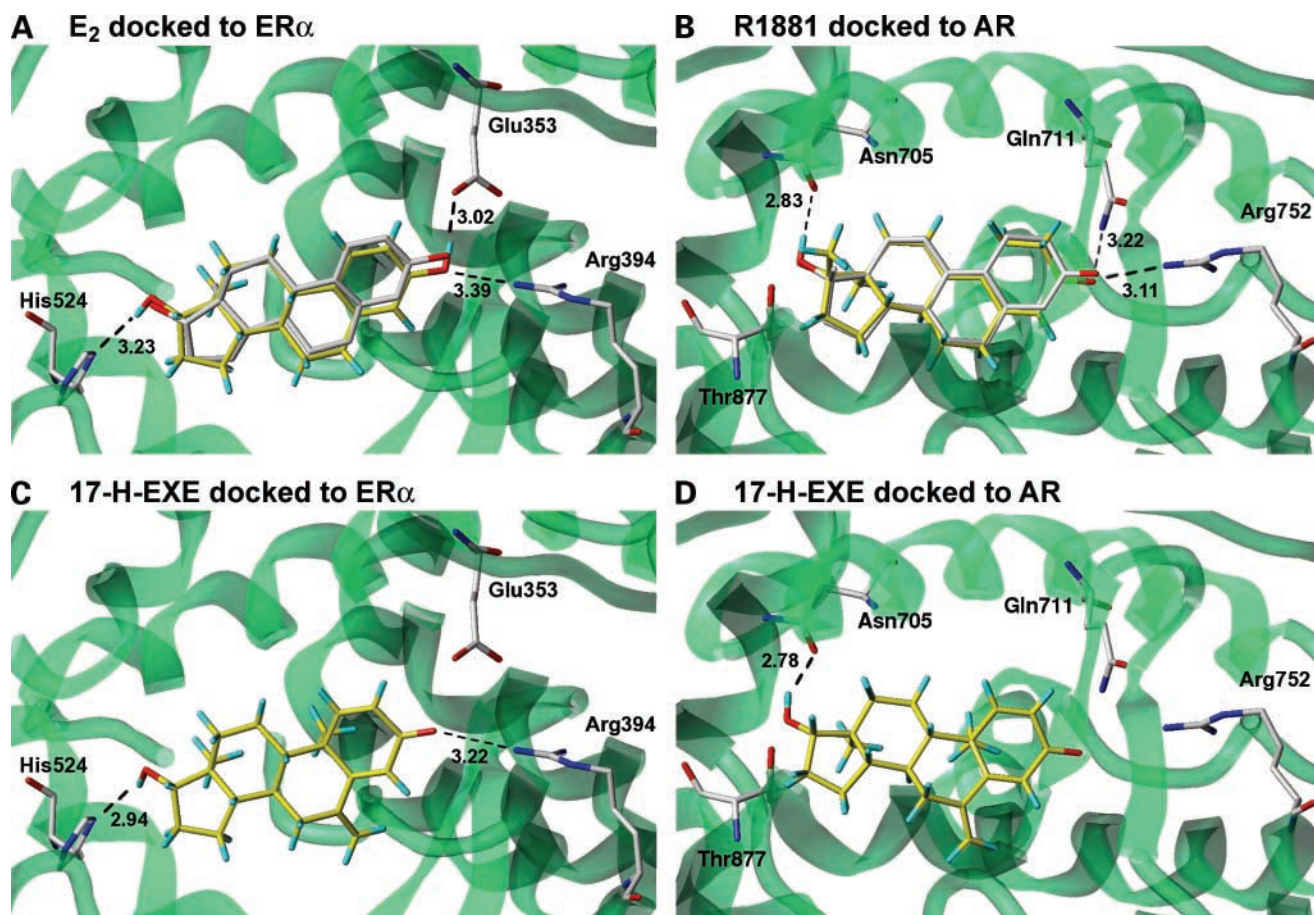


Figure 5. Intermolecular interactions of ligands complexed with ER α and AR by computer docking. **A**, superposition of E₂ from the X-ray crystal structure (*gray*) and modeled E₂ (*yellow*) docked to ER α . **B**, superposition of R1881 from the crystal structure (*gray*) and modeled R1881 (*yellow*) docked to AR. **C**, modeled 17-hydroexemestane docked to ER α . **D**, modeled 17-hydroexemestane docked to AR. *Cyan, red, and blue*, hydrogen, oxygen, and nitrogen atoms, respectively. *Green*, carbon backbone of the protein. Hydrogens from the X-ray crystal conformations of E₂ (**A**) and R1881 (**C**) were omitted. H-bonds were shown to the modeled compound conformations only. *Dashed lines*, intermolecular H-bonds up to 3.5 Å; their length in angstroms is indicated.

12 months of AI therapy, exemestane may be associated with slower rates of BMD loss compared with nonsteroidal AIs. Furthermore, although not directly comparable, the fracture rate per 1,000 woman-years in the ATAC trial was 22.6 for anastrozole and 15.6 for tamoxifen (1), whereas in the IES trial, the incidence rate per 1,000 woman-years for multiple fractures was 19.2 for exemestane and 15.1 for tamoxifen (10). These results show that although both anastrozole and exemestane were associated with higher fracture rates than tamoxifen, they also suggest that exemestane may be associated with a lower fracture rate than anastrozole. Clinical trials now under way to directly compare the different AIs will hopefully provide clear results.

Androgens regulate growth of normal and neoplastic mammary cells in a cell type-specific manner, either by inhibiting or stimulating growth (44). However, the mechanisms by which androgens via AR regulate breast cancer growth remain elusive. Female AR knock-out mice exhibit decreased ductal branching and terminal end buds in prepubertal animals and retarded lobuloalveolar development in adult animals (45). Likewise, targeted disruption of AR in MCF-7 cells also leads to severe inhibition of proliferation (45). Epidemiologic analyses indicate a positive correlation between androgen levels and the incidence of breast cancer; meta-analysis from nine prospective studies showed that a doubling in testosterone concentrations in postmenopausal women translated into an increased relative risk of 1.42 unadjusted and 1.32 adjusted for E₂ (46). AR status in breast cancer associates with both positive and negative indicators and clinical outcome. AR expression has been found in 84% (47) to 91% (48) of clinical breast cancers, and associated with ER status, but has also been found in 49% of ER-negative tumors (49). Patients with tumors that coexpress AR with ER and progesterone receptor have shown longer disease-free survival (DFS) than patients whose tumors were negative for all three receptors (48), but AR protein levels have also served as an independent predictor of axillary metastases in multivariate analysis (47). Furthermore, AR expression has correlated with decreased histopathologic grade, greater age, and postmenopausal status, but also lymph node-positive status (50). In AR-positive/ER-negative tumors, AR expression again associated with positive and negative indicators/outcome such as increased age, postmenopausal status, and longer DFS but also tumor grade, tumor size, and HER-2/neu overexpression (49).

Patients who fail AI therapy, whether the AI was steroidal or nonsteroidal, likely harbor tumor cells that have been selected for growth in an estrogen-depleted environment and, hence, are not dependent on ER activity for survival. Not all androgens are metabolized by aromatase to estrogens; for instance, dihydrotestosterone cannot be converted to an estrogen by aromatase (44). Thus, a possible mechanism for failure of AI therapy in the clinic is androgen-stimulated breast cancer growth, a largely unrecognized alternative mechanism. We observed cellular proliferation of T47D cells in response to R1881 and 17-hydroxemestane, and these effects were blocked by

bicalutamide. Therefore, T47D cells contain a functional AR signaling pathway that promoted growth in the absence of estrogen. Because functional AR signaling could be etiologically involved in a subpopulation of clinical breast cancers, those patients who have AR-positive tumors and achieve high circulating levels of 17-hydroxemestane, yet whose disease progresses while on exemestane therapy, may respond to AR-based therapy such as the antiandrogen bicalutamide.

Acknowledgments

We thank Dr. Alan E. Wakeling and Dr. Barrington J.A. Furr for providing fulvestrant and bicalutamide, respectively. We also thank members of the Jordan laboratory for helpful discussions, and Dr. Jennifer L. Ariazi (GlaxoSmithKline, Collegeville, PA) for critical review of the manuscript.

References

- Howell A, Cuzick J, Baum M, et al. Results of the ATAC (Arimidex, Tamoxifen, Alone or in Combination) trial after completion of 5 years' adjuvant treatment for breast cancer. *Lancet* 2005;365:60–2.
- Jonat W, Gnant M, Boccardo F, et al. Effectiveness of switching from adjuvant tamoxifen to anastrozole in postmenopausal women with hormone-sensitive early-stage breast cancer: a meta-analysis. *Lancet Oncol* 2006;7:991–6.
- Coates AS, Keshaviah A, Thurlimann B, et al. Five years of letrozole compared with tamoxifen as initial adjuvant therapy for postmenopausal women with endocrine-responsive early breast cancer: update of study BIG 1–98. *J Clin Oncol* 2007;25:486–92.
- Goss PE, Ingle JN, Martino S, et al. Randomized trial of letrozole compared with tamoxifen as extended adjuvant therapy in receptor-positive breast cancer: updated findings from NCIC CTG MA.17. *J Natl Cancer Inst* 2005;97:1262–71.
- Coombes RC, Hall E, Gibson LJ, et al. A randomized trial of exemestane following tamoxifen as extended adjuvant therapy in postmenopausal women with primary breast cancer. *N Engl J Med* 2004;350:1081–92.
- Coombes RC, Kilburn LS, Snowdon CF, et al. Survival and safety of exemestane versus tamoxifen after 2–3 years' tamoxifen treatment (Intergroup Exemestane Study): a randomised controlled trial. *Lancet* 2007;369:559–70.
- Jordan VC, Brodie AM. Development and evolution of therapies targeted to the estrogen receptor for the treatment and prevention of breast cancer. *Steroids* 2007;72:7–25.
- Howell A, Clarke RB, Evans G, et al. Estrogen deprivation for breast cancer prevention. *Recent Results Cancer Res* 2007;174:151–67.
- Buzdar A, Howell A, Cuzick J, et al. Comprehensive side-effect profile of anastrozole and tamoxifen as adjuvant treatment for early-stage breast cancer: long-term safety analysis of the ATAC trial. *Lancet Oncol* 2006;7:633–43.
- Coleman RE, Banks LM, Girgis SI, et al. Skeletal effects of exemestane on bone-mineral density, bone biomarkers, and fracture incidence in postmenopausal women with early breast cancer participating in the Intergroup Exemestane Study (IES): a randomised controlled study. *Lancet Oncol* 2007;8:119–27.
- Perez EA, Josse RG, Pritchard KI, et al. Effect of letrozole versus placebo on bone mineral density in women with primary breast cancer completing 5 or more years of adjuvant tamoxifen: a companion study to NCIC CTG MA.17. *J Clin Oncol* 2006;24:3629–35.
- Eastell R, Hannon RA, Cuzick J, Dowsett M, Clack G, Adams JE. Effect of an aromatase inhibitor on bmd and bone turnover markers: 2-year results of the Anastrozole, Tamoxifen, Alone or in Combination (ATAC) trial (18233230). *J Bone Miner Res* 2006;21:1215–23.
- Morales L, Pans S, Paridaens R, et al. Debilitating musculoskeletal pain and stiffness with letrozole and exemestane: associated tenosynovial changes on magnetic resonance imaging. *Breast Cancer Res Treat* 2007;104:87–91.
- Mackey J, Gelmon K. Adjuvant aromatase inhibitors in breast cancer therapy: significance of musculoskeletal complications. *Curr Opin Oncol* 2007;19 Suppl 1:S9–18.

15. Goss PE, Qi S, Josse RG, et al. The steroidal aromatase inhibitor exemestane prevents bone loss in ovariectomized rats. *Bone* 2004;34:384–92.
16. Goss PE, Qi S, Cheung AM, Hu H, Mendes M, Pritzker KP. Effects of the steroidal aromatase inhibitor exemestane and the nonsteroidal aromatase inhibitor letrozole on bone and lipid metabolism in ovariectomized rats. *Clin Cancer Res* 2004;10:5717–23.
17. Lonning PE, Geisler J, Krag LE, et al. Effects of exemestane administered for 2 years versus placebo on bone mineral density, bone biomarkers, and plasma lipids in patients with surgically resected early breast cancer. *J Clin Oncol* 2005;23:5126–37.
18. Coleman RE, Group AT. Effect of anastrozole on bone mineral density: 5-year results from the 'Arimidex,' Tamoxifen, Alone or in Combination (ATAC) trial. *J Clin Oncol (Meeting Abstracts)* 2006;24:511.
19. Love RR, Mazess RB, Barden HS, et al. Effects of tamoxifen on bone mineral density in postmenopausal women with breast cancer. *N Engl J Med* 1992;326:852–6.
20. Cummings SR, Browner WS, Bauer D, et al. Endogenous hormones and the risk of hip and vertebral fractures among older women. *N Engl J Med* 1998;339:733–8.
21. Hofbauer LC, Khosla S. Androgen effects on bone metabolism: recent progress and controversies. *Eur J Endocrinol* 1999;140:271–86.
22. Miki Y, Suzuki T, Hatori M, et al. Effects of aromatase inhibitors on human osteoblast and osteoblast-like cells: a possible androgenic bone protective effects induced by exemestane. *Bone* 2007;40:876–87.
23. Lea CK, Flanagan AM. Physiological plasma levels of androgens reduce bone loss in the ovariectomized rat. *Am J Physiol* 1998;274:E328–35.
24. Tobias JH, Gallagher A, Chambers TJ. 5 α -Dihydrotestosterone partially restores cancellous bone volume in osteopenic ovariectomized rats. *Am J Physiol* 1994;267:E853–9.
25. Buchanan JR, Hospodar P, Myers C, Leuenberger P, Demers LM. Effect of excess endogenous androgens on bone density in young women. *J Clin Endocrinol Metab* 1988;67:937–43.
26. Dixon JE, Rodin A, Murby B, Chapman MG, Fogelman I. Bone mass in hirsute women with androgen excess. *Clin Endocrinol (Oxf)* 1989;30:271–7.
27. Riggs BL, Jowsey J, Goldsmith RS, Kelly PJ, Hoffman DL, Arnaud CD. Short- and long-term effects of estrogen and synthetic anabolic hormone in postmenopausal osteoporosis. *J Clin Invest* 1972;51:1659–63.
28. Barrett-Connor E, Young R, Notelovitz M, et al. A two-year, double-blind comparison of estrogen-androgen and conjugated estrogens in surgically menopausal women. Effects on bone mineral density, symptoms and lipid profiles. *J Reprod Med* 1999;44:1012–20.
29. di Salle E, Giudici D, Ornati G, et al. 4-Aminoandrostenedione derivatives: a novel class of irreversible aromatase inhibitors. Comparison with FCE 24304 and 4-hydroxyandrostenedione. *J Steroid Biochem Mol Biol* 1990;37:369–74.
30. Evans TR, Di Salle E, Ornati G, et al. Phase I and endocrine study of exemestane (FCE 24304), a new aromatase inhibitor, in postmenopausal women. *Cancer Res* 1992;52:5933–9.
31. Pfizer Inc. Product information: Aromasin, exemestane tablets. New York, NY 10017; 2007.
32. Pink JJ, Jordan VC. Models of estrogen receptor regulation by estrogens and antiestrogens in breast cancer cell lines. *Cancer Res* 1996;56:2321–30.
33. Ariazi EA, Kraus RJ, Farrell ML, Jordan VC, Mertz JE. Estrogen-related receptor α 1 transcriptional activities are regulated in part via the ErbB2/HER2 signaling pathway. *Mol Cancer Res* 2007;5:71–85.
34. Abdelrahim M, Ariazi E, Kim K, et al. 3-Methylcholanthrene and other aryl hydrocarbon receptor agonists directly activate estrogen receptor α . *Cancer Res* 2006;66:2459–67.
35. Bauer JA, Thompson TA, Church DR, Ariazi EA, Wilding G. Growth inhibition and differentiation in human prostate carcinoma cells induced by the vitamin D analog 1 α ,24-dihydroxyvitamin D₂. *Prostate* 2003;55:159–67.
36. Warnmark A, Treuter E, Gustafsson JA, Hubbard RE, Brzozowski AM, Pike AC. Interaction of transcriptional intermediary factor 2 nuclear receptor box peptides with the coactivator binding site of estrogen receptor α . *J Biol Chem* 2002;277:21862–8.
37. He B, Gampe RT, Jr., Kole AJ, et al. Structural basis for androgen receptor interdomain and coactivator interactions suggests a transition in nuclear receptor activation function dominance. *Mol Cell* 2004;16:425–38.
38. Brzozowski AM, Pike AC, Dauter Z, et al. Molecular basis of agonism and antagonism in the oestrogen receptor. *Nature* 1997;389:753–8.
39. Matias PM, Donner P, Coelho R, et al. Structural evidence for ligand specificity in the binding domain of the human androgen receptor. Implications for pathogenic gene mutations. *J Biol Chem* 2000;275:26164–71.
40. Fang H, Tong W, Shi LM, et al. Structure-activity relationships for a large diverse set of natural, synthetic, and environmental estrogens. *Chem Res Toxicol* 2001;14:280–94.
41. Fang H, Tong W, Branham WS, et al. Study of 202 natural, synthetic, and environmental chemicals for binding to the androgen receptor. *Chem Res Toxicol* 2003;16:1338–58.
42. Wolf DA, Herzinger T, Hermeking H, Blaschke D, Horz W. Transcriptional and posttranscriptional regulation of human androgen receptor expression by androgen. *Mol Endocrinol* 1993;7:924–36.
43. Zhou ZX, Lane MV, Kempainen JA, French FS, Wilson EM. Specificity of ligand-dependent androgen receptor stabilization: receptor domain interactions influence ligand dissociation and receptor stability. *Mol Endocrinol* 1995;9:208–18.
44. Somboonporn W, Davis SR. Testosterone effects on the breast: implications for testosterone therapy for women. *Endocr Rev* 2004;25:374–88.
45. Yeh S, Hu Y-C, Wang P-H, et al. Abnormal mammary gland development and growth retardation in female mice and MCF7 breast cancer cells lacking androgen receptor. *J Exp Med* 2003;198:1899–908.
46. Group EHaBCC. Endogenous sex hormones and breast cancer in postmenopausal women: reanalysis of nine prospective studies. *J Natl Cancer Inst* 2002;94:606–16.
47. Soreide JA, Lea OA, Varhaug JE, Skarstein A, Kvinnsland S. Androgen receptors in operable breast cancer: relation to other steroid hormone receptors, correlations to prognostic factors and predictive value for effect of adjuvant tamoxifen treatment. *Eur J Surg Oncol* 1992;18:112–8.
48. Kuenen-Boumeester V, Van der Kwast TH, Claassen CC, et al. The clinical significance of androgen receptors in breast cancer and their relation to histological and cell biological parameters. *Eur J Cancer* 1996;32A:1560–5.
49. Agoff SN, Swanson PE, Linden H, Hawes SE, Lawton TJ. Androgen receptor expression in estrogen receptor-negative breast cancer. Immunohistochemical, clinical, and prognostic associations. *Am J Clin Pathol* 2003;120:725–31.
50. Bieche I, Parfait B, Tozlu S, Lidereau R, Vidaud M. Quantitation of androgen receptor gene expression in sporadic breast tumors by real-time RT-PCR: evidence that MYC is an AR-regulated gene. *Carcinogenesis* 2001;22:1521–6.